

Wind Stress induced by Sea Waves

Part 2: Effect of Thermal Stratification on Wave Growth by Wind

Project: NAUTILUS

Werkdocument: RIKZ/OS/2002.125x



In opdracht van:

Directie Noordzee
Directie Zuid-Holland
Directie Zeeland
Directie Noord-Holland
Gemeentelijk Havenbedrijf Rotterdam
Directoraat-Generaal Water

WIND STRESS INDUCED BY SEA WAVES

Part 2: Effect of thermal stratification on wave growth by wind

Projecten : NAUTILUS en
 HR-ONTWIKKELING

Werkdocument : RIKZ/OS/2002.125x

Datum : December 2002

Auteur : A.C. Radder

WIND STRESS INDUCED BY SEA WAVES

Part 2: Effect of thermal stratification on wave growth by wind

A.C. Radder

Abstract

The purpose of Part 2 of the present report is threefold:

- (i) to deliver a more fundamental analysis in support of the CL-theory, as applied in Part 1 to the problem of momentum transfer between air and sea;
- (ii) to extend the theory by including a convection-diffusion equation for turbulent heat transfer, to describe the effect of the resulting thermal stratification on wave growth by wind;
- (iii) to explain the effect of physical processes as shoaling and swell on wave growth and roughness of the sea surface.

1. Introduction

Observations show that stability (*c.q.* gustiness) of the atmospheric boundary layer (ABL) due to differences in temperature between air and sea can affect the growth of surface waves by wind significantly: in unstable conditions wind-wave growth is enhanced whereas in stable conditions it is reduced (*cf.* van den Boogaard *et al.* 1991, p.11; Young 1998; van Vledder 1999; Jones and Toba 2001; Sullivan and McWilliams 2002). Usually, this effect is accounted for by the *Monin-Obukhov* similarity theory, which relates the wind profile to the roughness of the sea surface and the stability of the atmosphere, through a parametric description of the heat flux involved. However, the theory is questioned on the assumption that its parameter set is complete, regarding the influence of the height of the ABL on surface layer characteristics (Johansson *et al.* 2001; McNaughton and Brunet 2002). There exists an extensive literature on measurements of wind stress over oceans and shallow seas; however, the data show a significant scatter when the drag coefficient is presented as a function of the mean wind speed at a reference height. While this scatter can be explained partly as a consequence of the age of the wave field (*cf.* Bonekamp *et al.* 2002; Lin *et al.* 2002), other parameters play a part, as significant wave height, steepness, and spectral shape (Taylor and Yelland 2001). Note that atmospheric roll vortices, as observed by Vandemark *et al.* (2001), induce fluctuations in local wind speed, and thus variations in sea surface roughness and wind stress. Further theoretical development is invaluable to understand the influence of the various physical processes.

The *Craik-Leibovich* (CL)-theory, which describes the interaction between waves and mean flows, has been employed by Radder (2001; henceforth referred to as Part 1) to develop a model for the wave-induced wind stress, the wave growth by wind and the related roughness of the sea surface. Due to the CL2-instability mechanism involved, roll-patterns appear in the atmospheric boundary layer above the sea surface; a ‘principle of maximum energy transfer’ is then invoked, to establish a relation between the roughness parameter and the friction velocity; as a consequence, both the growth rate and the mean drag attain maximum values for a given wind and wave field.

In this second part of the report, the theory is extended by adding to the existing continuity and momentum equations a convection-diffusion equation for turbulent heat transfer, and applying the Boussinesq approximation (§2). In support of the theory of Part 1, a more fundamental approach is presented in §3 by a time-scale analysis: changes in the ABL due to the interaction between wind and surface waves appear to be fast in comparison with the time scale associated with the evolution of the waves. After a linear stability analysis (§4), the effect of atmospheric stability - owing to differences in temperature between air and sea - on the growth rate, as a function of a *Richardson number*, is estimated in §5. Some properties of an analytical and a numerical model are given in §6. Finally, §7 presents conclusions and recommendations.

2. Governing equations. Energy balance

The extended CL-equations for a thermally stratified turbulent flow in the atmospheric boundary layer are (Leibovich 1983; Arya 2001; Dingemans 2001; Part 1, §2)

$$D_{\pi} \mathbf{U}_{\pi} / Dt + \nabla P_T = \nabla \cdot \Sigma / \rho_a + (\mathbf{U}_{\pi} + \mathbf{P}_S) \times \Omega_C + \mathbf{P}_S \times \Omega - \beta_T \mathbf{g} \theta + \mathcal{O}(a^4) , \quad (1a)$$

$$D\Theta / Dt = \nabla \cdot (\alpha_T \nabla \Theta) , \quad (1b)$$

$$\nabla \cdot \mathbf{U} = 0 . \quad (1c)$$

Herein,

$\mathbf{U}_{\pi} \equiv \mathbf{U} - \boldsymbol{\pi}$, with $\boldsymbol{\pi} = \mathbf{P}_S - \mathbf{U}_S$, \mathbf{U} is the mean Eulerian velocity,

\mathbf{P}_S the pseudo-momentum, \mathbf{U}_S the (generalized) Stokes drift,

P_T the generalized pressure, $\Sigma = 2 \rho_a \nu_T \mathbf{D}$ the Reynolds stress tensor,

ρ_a the air density, ν_T a (turbulent) eddy viscosity,

$\Omega = \nabla \times \mathbf{U}$ the mean vorticity,

Ω_C the Coriolis rotation vector,

equal to *twice* the angular velocity of the earth,

$\mathbf{g} \equiv (0, 0, -g)$ the acceleration of gravity,

Θ the mean virtual potential air temperature,

θ the fluctuating virtual potential air temperature,

$\beta_T = -\rho_a^{-1} \partial \rho_a / \partial \Theta$ the coefficient of thermal expansion,

α_T a (turbulent) eddy diffusivity of heat,

and a a measure of wave amplitude.

A definition of the virtual $c.q.$ potential temperature, expressing the influence of humidity $c.q.$ pressure on the air temperature, can be found in Arya (2001, Ch. 5) and Csanady (2001).

Besides the vortex force $\mathbf{P}_S \times \Omega$ equation (1a) contains the buoyancy force $-\beta_T \mathbf{g} \theta$ due to temperature fluctuations; the evolution of the temperature Θ is governed by the convection-diffusion equation (1b), with velocity \mathbf{U} satisfying the continuity equation (1c).

The following simplifications and assumptions were made in the derivation of (1):

- (i) the air is incompressible, and the Boussinesq approximation is applied;
- (ii) the air-wave field is irrotational outside its boundary layers, and of small amplitude a ;
- (iii) the water-wave field is homogeneous within a convection cell;
- (iv) slow mean-flow and wave variations in the horizontal plane are considered.

Assuming horizontally homogeneous flow conditions in the atmospheric boundary layer, $\mathbf{U} \equiv \{U(z,t), V(z,t), 0\}$, $\mathbf{P}_S \equiv (P_S, Q_S, 0)$, $\Theta \equiv \Theta(z,t)$, with wave-induced disturbance $\{\mathbf{u}; \theta\} \equiv \{u, v, w; \theta\}$, air density $\rho_a(z)$ and eddy viscosity $\nu_T(z)$, the wave-induced *Reynolds-Orr* energy-balance equation is (cf. Arya 2001, §9.1; Part 1, §3):

$$dK/dt = - \int_0^h dz \rho_a \{ \frac{1}{2} \nu_T \langle 2\mathbf{d}; 2\mathbf{d} \rangle + \langle w\mathbf{u} \rangle \cdot \partial(\mathbf{U} + \mathbf{U}_S) / \partial z - \beta_T g \langle w\theta \rangle \} - dE/dt + \mathcal{O}(a^3, a^2 \mu^2), \quad (2)$$

where $K = \frac{1}{2} \int_0^h dz \rho_a \langle \mathbf{u} \cdot \mathbf{u} \rangle$ is the kinetic energy of the disturbance, $\mathbf{d} \equiv \{d_{ij}\} = \frac{1}{2} \{\partial u_i / \partial x_j + \partial u_j / \partial x_i\}$ the deformation tensor of the velocity disturbance \mathbf{u} , h indicates the height of the arising convection cell, $\langle \dots \rangle$ denotes averaging over horizontal planes of a convection cell, and E is the mean wave-energy per unit area of the sea surface. The parameter $\mu \ll 1$ indicates that the shear of the disturbance is assumed to be small compared with the shear of the mean flow.

Note that the buoyancy flux $\beta_T g \langle w\theta \rangle$, when scaled with $(U^*)^3$, where U^* the *friction velocity* of the wind, is comparable with the Obukhov scale height L ; while the velocity is scaled with U^* , the temperature is scaled with the *friction temperature* Θ^* .

The wind and temperature profiles are related to the wave-induced fluxes of momentum and heat, and the corresponding eddy diffusivities; in equilibrium-flow state, from (1a) and (1b) the mean wind profile $\mathbf{U}(z)$ and the mean temperature profile $\Theta(z)$ are obtained as

$$\partial \mathbf{U} / \partial z \cong (\langle w\mathbf{u} \rangle + |\mathbf{U}^*| \mathbf{U}^*) / \nu_T, \quad (3)$$

$$\text{and} \quad \partial \Theta / \partial z \cong (\langle w\theta \rangle + |\mathbf{U}^*| \Theta^*) / \alpha_T, \quad (4)$$

with $|\mathbf{U}^*| = \sqrt{(U^*U^* + V^*V^*)}$, $\text{sign}(\mathbf{U}^*) = \text{sign}(\partial \mathbf{U} / \partial z)_0$ and $\text{sign}(\Theta^*) = \text{sign}(\partial \Theta / \partial z)_0$.

In these expressions, the influence of the Coriolis force is neglected, assuming a ‘*constant stress layer*’ model; otherwise, a damping function $f_D(z)$ can be introduced to achieve that the total shear stress $\tau = \rho_a |\mathbf{U}^*| \mathbf{U}^*$ decays with height and eventually vanishes at the top of the surface layer.

Accordingly, the eddy diffusivities $\nu_T(z)$ and $\alpha_T(z)$, as functions of geometry and flow parameters, will be specified later on (§4.4). Note that (3) expresses the partitioning of the total stress into a wave-induced stress and a turbulent viscous stress (cf. Uz *et al.* 2002).

In order to proceed with the energy balance (2) to develop a subcell-scale model for the wave-induced Reynolds-stress $\langle w\mathbf{u} \rangle$, it is necessary to distinguish between the time scales of the various physical processes involved; in the next section, a time-scale analysis is given, and a ‘principle of maximum energy transfer’ is formulated as a *hypothesis*, based on the optimum theory of turbulent shear flow.

3. Time-scale analysis. Optimum theory of turbulent shear flow

The present CL-model employs two time scales (see figure 1; *cf.* also Part 1, p. 6):

1) on the ‘fast’ time scale t , secondary circulations are formed in the atmospheric boundary layer (‘roll vortices’; size ± 1 km), through an instability mechanism in the interaction between wind and surface waves, with given wave field; as a consequence, an *inverse energy cascade* occurs from small-scale to large-scale circulations;

2) on the ‘slow’ time scale T , nonlinear transfer of energy is assumed to occur from these large-scale circulations to turbulent eddies on small scales, through vortex stretching (the *turbulent energy cascade*); by this process the wave field is capable to absorb the released energy, implying wave growth.

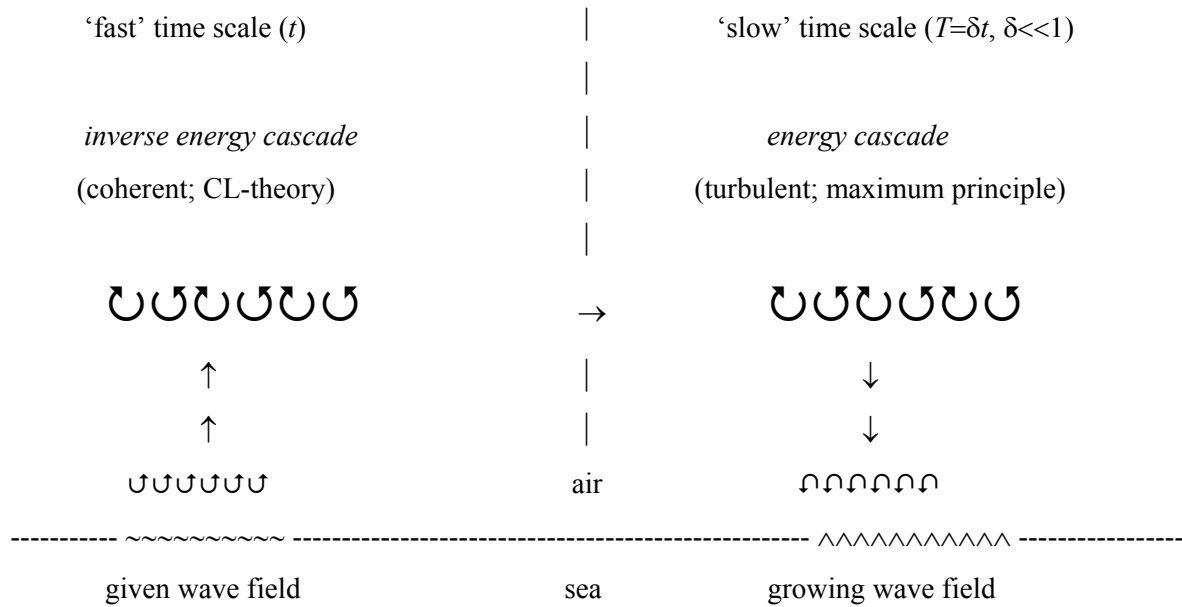


figure 1

The *first* process is described by the extended Craik-Leibovich theory, which is a well established theory defining the interaction between waves and mean flows:

- Leibovich and Paolucci (1980) used the extended CL-theory with constant eddy diffusivities to compute the development of a mixed layer in a thermally stratified ocean, with imposed wind stress and surface-wave field. The resulting convective motions appear to cascade energy from small-scale to large-scale (Langmuir) circulations.
- Araujo *et al.* (2001) employed a (k - ϵ) turbulence model coupled to the CL-equations to investigate the enhanced turbulence observed beneath air-water interfaces and the presence of

organized structures like Langmuir circulations. A good agreement was found between numerical results and experimental data from a wind-wave channel.

- Phillips *et al.* (1996, 1999) studied the CL2 instability mechanism in case of a boundary layer flow over wavy terrain, with $O(1)$ shear; then, the pseudo-momentum replaces the Stokes drift, and wave distortion appears to diminish the instability. (Note that the latter effect is neglected in the present application to the atmosphere.)

The *second* process requires some further explanation. In the theory of turbulence, variational methods have been employed to derive rigorous upper bounds on certain global flow quantities that characterize statistically steady turbulent flows. To this end, various approaches have been developed in the past:

- the upper-bound theory, by Malkus (1956) and Howard (1972);
- the optimum theory, by Busse (1978);
- the background flow method, by Doering and Constantin (1992).

In this work, global transport quantities like momentum-, heat- and mass-fluxes across turbulent boundary layers are investigated and found to become extremal, depending on the constraints (such as continuity and boundary conditions) imposed on the admitted velocity fields. Under statistically steady conditions or long-time averaging, this approach is equivalent to bounding the energy dissipation rate (*cf.* Kerswell 2002 for references on various applications). By adding further constraints on the flow and using different dissipation functionals, the theory has been extended and generalized by Malkus and Smith (1989), Nicodemus *et al.* (1998), and Kerswell (2002), in order to close the gap between the theoretical and the experimentally measured dissipation rates.

Unfortunately, as has been noted by Kerswell (2002), these variational problems involve heuristic assumptions which cannot be traced back to the Navier-Stokes equations. Nevertheless, to quote Busse (1978): ‘In principle it is possible to conceive a hierarchy of constraints such that the bounds approach the extremal values assumed by the actual solutions of the equations of motion, and thus can be brought closer and closer to the observed values’.

Remark. The foregoing approach is consistent with the *constructal theory* developed and described by Bejan (2000): in engineering and in nature, flow systems with geometric structure tend to optimal distribution of internal flow resistance. This principle applies to a wide range of topics, including mechanical, thermal and turbulent structure. Examples are:

- the growth rate of the mixing region in shear layers, through time-minimization analysis;
- the optimization of thermal resistance in Rayleigh-Bénard convection, through the maximization of the heat transfer rate.

In the present problem, we are concerned with wave-induced atmospheric roll vortices, which contain most of the turbulent kinetic energy of the atmospheric boundary layer (Lykossov 2001). The corresponding energy-balance equation (2) becomes, in equilibrium-flow state,

$$d(K+E)/dt = - \int_0^h dz \rho_a \{ \frac{1}{2} v_T \langle 2\mathbf{d}:2\mathbf{d} \rangle + \langle w\mathbf{u} \rangle \cdot \partial(U+\mathbf{U}_S)/\partial z - \beta_T g \langle w\theta \rangle \} = 0 , \quad (5)$$

where the terms on the right-hand side represent successively the dissipation rate, the production due to shear and the production / destruction due to buoyancy. Note that besides the integral constraint of streamwise vorticity, further constraints can be imposed by a suitable choice of (parameters of) the eddy diffusivities of momentum and heat, $v_T(z)$ and $\alpha_T(z)$.

In order to obtain an optimum solution to the problem, we invoke the following

Hypothesis. The wave-induced dissipation rate $D_v \equiv \frac{1}{2} \int_0^h dz \rho_a v_T \langle 2\mathbf{d}:2\mathbf{d} \rangle$, conceived as a functional of steady-state mean-flow properties *c.q.* parameters, attains a maximum value for a given wave field, at the expense of the kinetic energy K : $D_{v, \max} = - dK/dt$.

It follows that the energy transferred from the atmosphere to the wave motion tends to a maximum as well:

$$dE/dt = - \int_0^h dz \rho_a \{ \langle w\mathbf{u} \rangle \cdot \partial(U+\mathbf{U}_S)/\partial z - \beta_T g \langle w\theta \rangle \} \Big|_{\max} . \quad (6)$$

This *principle of maximum energy transfer* is consistent with a hypothesis postulated by Oberlack (2001): *The mean velocity in an incompressible turbulent flow establishes a maximum degree of symmetry consistent with the Reynolds-averaged Navier-Stokes equations and the initial and boundary conditions.* In the present case, the development of roll vortices in the atmospheric boundary layer involves symmetry breaking of the mean flow; according to the hypothesis, the flow thus exhibits a strong tendency towards a higher degree of symmetry, *i.e.* to reduce the strength of the vortices by energy transfer to surface waves.

Owing to this maximum principle, the roughness parameter and friction velocity can be determined, and the wind drag and wave growth established, using the flux-profile relationships (3) and (4).

4. Linear stability analysis. Equilibrium solution

When the disturbance (\mathbf{u}, θ) is sufficiently small, linearization is permitted, and in the present approximation, $\mathbf{u} \equiv \{u, v, w\}$ and θ obey the equations (cf. also Dingemans 2001, § 3.3):

$$\partial u / \partial t + U_\pi \partial u / \partial x + V_\pi \partial u / \partial y + w \partial U_\pi / \partial z + 1/\rho_a \partial p / \partial x = 1/\rho_a (\nabla \cdot \boldsymbol{\sigma})_x + Q_S \omega_z , \quad (7a)$$

$$\partial v / \partial t + U_\pi \partial v / \partial x + V_\pi \partial v / \partial y + w \partial V_\pi / \partial z + 1/\rho_a \partial p / \partial y = 1/\rho_a (\nabla \cdot \boldsymbol{\sigma})_y - P_S \omega_z , \quad (7b)$$

$$\partial w / \partial t + U_\pi \partial w / \partial x + V_\pi \partial w / \partial y + 1/\rho_a \partial p / \partial z = 1/\rho_a (\nabla \cdot \boldsymbol{\sigma})_z + P_S \omega_y - Q_S \omega_x + \beta_T g \theta , \quad (7c)$$

$$\partial \theta / \partial t + U \partial \theta / \partial x + V \partial \theta / \partial y + w \partial \Theta / \partial z = \nabla \cdot (\alpha_T \nabla \theta) , \quad (7d)$$

$$\text{with continuity equation} \quad \partial u / \partial x + \partial v / \partial y + \partial w / \partial z = 0 . \quad (8)$$

The linear stability problem can be analysed using a *long-wave* (or: *shallow-water*) asymptotic expansion in powers of the small parameter ε ; correspondingly, mixed boundary conditions on u , v , and w are chosen:

$$\partial(u; v) / \partial z \pm \alpha_C (u; v) = 0 , \quad (9a)$$

$$w = 0 , \quad (9b)$$

at the mean free surface $z = 0$ and at the cell height $z = h$, with parameter $\alpha_C = \mathcal{O}(\varepsilon^4)$.

Remark. The free-slip boundary conditions $\partial u / \partial z = \partial v / \partial z = 0$ (known as ‘*constant stress model*’) lead to unstable modes of infinite wavelength; therefore, Cox and Leibovich (1993) and Cox (1997) considered the mixed boundary conditions $\partial(u; v) / \partial z \pm \alpha_C (u; v) = 0$, with $\alpha_C = \mathcal{O}(\varepsilon^4)$. However, for the present purpose, only second order results in ε are needed, so the boundary conditions $\partial u / \partial z = \partial v / \partial z = 0$ are sufficient to this end.

For the boundary conditions on θ at $z = 0$ and $z = h$, we have several alternatives:

- 1) condition of constant heat flux H_0 , $\partial \theta / \partial z = -\partial \Theta / \partial z + H_0 / \alpha_T$;
- 2) mixed boundary condition, $\partial \theta / \partial z \pm \gamma_C \theta = 0$ (Cox and Leibovich, 1993).

As special cases, we have from 1) the adiabatic condition: $H_0 = 0$, and from 2) the isothermal condition: $\theta = 0$ (i.e. $\gamma_C = \infty$), and the condition: $\partial \theta / \partial z = 0$ (i.e. $\gamma_C = 0$). In the following, we consider the two extreme cases $\theta = 0$ (§4.1) and $\partial \theta / \partial z = 0$ (§4.2). [Note that in the present approximation (to second order in ε) the latter condition holds as well when $\gamma_C = \mathcal{O}(\varepsilon^4)$.]

Employing the *shallow-water* expansion (Proctor, 1981; Cox and Leibovich, 1993; Cox, 1997)

$$(\mathbf{u}, \theta; [dp/\rho_a]) \approx (\mathbf{u}_0 + \varepsilon \mathbf{u}_1 + \dots; \theta_0 + \varepsilon \theta_1 + \dots; p_0 + \varepsilon p_1 + \dots) \exp\{i\varepsilon(kx + ly) + \varepsilon(\sigma_1 + \varepsilon \sigma_2 + \dots)t\}, \quad (10)$$

with $\mathbf{u}_i(z)$, $\theta_i(z)$ and $p_i(z)$ functions of z alone, and k, l scaled cell wave numbers, $\mathcal{O}(1)$, and upon substituting (10) into (7,8), we are able to solve the equations that result at successive orders in ε , taking into account the boundary conditions (9) at each order in the expansion.

4.1. The isothermal boundary condition $\theta = 0$

From the details given in appendix A, we obtain the following results: u_0, v_0 are constants, generally $\neq 0$, satisfying the relation $ku_0 + lv_0 = 0$; $w_0 \equiv w_1 \equiv 0$; $\theta_0 \equiv \theta_1 \equiv 0$; $w_2(z)$ and $\theta_2(z)$ are given by the solution of:

$$\partial_z(v_T \partial_z^2 w_2) = [l(\underline{P}_S - P_S) - k(\underline{Q}_S - Q_S)](lu_0 - kv_0), \quad (11a)$$

$$\text{and} \quad w_2 \partial_z \Theta = \partial_z(\alpha_T \partial_z \theta_2), \quad (11b)$$

with boundary conditions: $w_2 = 0$, $\partial_z^2 w_2 = 0$, and $\theta_2 = 0$ at $z = 0$ and $z = h$.

Introducing the velocity amplitude A_0 , cell wave-number modulus $\kappa_C = \sqrt{k^2 + l^2}$, and orientation $q = k/l$, let

$$lu_0 - kv_0 = \kappa_C A_0, \quad w_2(z) = \kappa_C^2 A_0 m_0(z), \quad \theta_2(z) = \kappa_C^2 A_0 \theta_m(z), \quad (12)$$

then (11a,b) become

$$\partial_z(v_T \partial_z^2 m_0) = [(\underline{P}_S - P_S) - q(\underline{Q}_S - Q_S)]/\sqrt{1+q^2}, \quad (13a)$$

$$\text{and} \quad \partial_z(\alpha_T \partial_z \theta_m) = m_0 \partial_z \Theta, \quad (13b)$$

with boundary conditions: $m_0 = 0$, $\partial_z^2 m_0 = 0$, and $\theta_m = 0$ at $z = 0$ and $z = h$.

In conclusion, in the present approximation we have the same equation (13a) for the wave-induced disturbance \mathbf{u} as in case of neutral stability conditions (*cf.* Dingemans 2001, § 4.2); the induced fluctuating temperature $\theta \equiv \theta_2(z)$ depends on the gradient of the mean temperature $\partial_z \Theta$, and is given by the solution of (13b).

4.2. The boundary condition $\partial \theta / \partial z = 0$

The details of this case are given in appendix B: u_0, v_0 and θ_0 are constants, generally $\neq 0$; $ku_0 + lv_0 = 0$; $w_0 \equiv w_1 \equiv 0$; $w_2(z)$ and θ_0 are given by the solution of:

$$\partial_z (v_T \partial_z^2 w_2) = [l(P_S - P_S) - k(Q_S - Q_S)](lu_0 - kv_0) + (k^2 + l^2) \beta_T \theta_0 g(z - h/2), \quad (14a)$$

$$\int_0^h dz [(k^2 + l^2)(\alpha_T - v_T) - w_2 \partial_z (IU - kV)/(lu_0 - kv_0)] \theta_0 = - \int_0^h dz w_2 \partial_z \Theta, \quad (14b)$$

with boundary conditions: $w_2 = 0$, $\partial_z^2 w_2 = 0$, at $z = 0$ and $z = h$.

Now with (12) we obtain

$$\partial_z (v_T \partial_z^2 m_0) = [(P_S - P_S) - q(Q_S - Q_S)]/\sqrt{1+q^2} + g \beta_T (z - h/2) \theta_m, \quad (15a)$$

$$\text{and} \quad \int_0^h dz [(v_T - \alpha_T) + m_0 \partial_z (U - qV)/\sqrt{1+q^2}] \theta_m = \int_0^h dz m_0 \partial_z \Theta, \quad (15b)$$

which form a coupled set of equations for $m_0(z)$ and $\theta_m = \theta_0/A_0$, with boundary conditions:

$m_0 = 0$, $\partial_z^2 m_0 = 0$, at $z = 0$ and $z = h$. Note that the pressure fluctuation, averaged over height, is given by:

$$\underline{p}_0 = (\underline{P}_S - q\underline{Q}_S) A_0 / \sqrt{1+q^2}. \quad (15c)$$

4.3. Choice of boundary condition. Equilibrium solution

The isothermal boundary condition (§4.1) results in an expression for the heat flux $\langle w\theta \rangle \sim \frac{1}{2} w_2 \theta_2$, where $w_2(z)$ and $\theta_2(z)$ are given by the solutions of (11a) resp. (11b). However, this approach turns out to suffer from the following disadvantages:

- the heat flux $\frac{1}{2} w_2 \theta_2$ depends on the cell wave-number modulus κ_C , which is unknown *a priori* and must be found by carrying on the asymptotic expansion up to $\mathcal{O}(\varepsilon^4)$, cf. Cox (1997);
- the fluctuating temperature $\theta_2(z)$ has to be found from the solution of the diffusion equation (11b), whereas $w_2(z)$, given as the solution of (11a) does not explicitly depend on θ_2 .

Therefore, in the following we will go on with the results from the boundary condition $\partial\theta/\partial z = 0$, namely the expression $\langle w\theta \rangle \sim \frac{1}{2} w_2 \theta_0$, and consider the corresponding coupled set of equations for $w_2(z)$ and θ_0 (or, equivalently, $m_0(z)$ and θ_m) as presented in §4.2.

The wave-induced wind stress and heat flux are now given by

$$\langle wu \rangle = \frac{1}{2} [(\alpha - \beta)/\gamma] m_0(z) / \sqrt{1+q^2}, \quad \langle wv \rangle = -q \langle wu \rangle, \quad (16a,b)$$

$$\langle w\theta \rangle = \frac{1}{2} [(\alpha - \beta)/\gamma] \theta_m m_0(z), \quad (16c)$$

when $\alpha > \beta$; otherwise, a threshold for onset of stability exists, and $\langle wu \rangle = \langle wv \rangle = \langle w\theta \rangle \equiv 0$.

From (16), the heat flux $\langle w\theta \rangle$ can be related to the momentum flux $\langle wu \rangle$,

$$\langle w\theta \rangle = [\langle wu \rangle - q \langle wv \rangle] \theta_m / \sqrt{1+q^2}. \quad (17)$$

The profile $m_0(z)$ and the constant θ_m are given by the solution of (15a,b), while the coefficients α , β and γ are evaluated in appendix C. *Result:* to leading order, the wave-induced wind stress and heat flux in equilibrium-flow state are independent of the cell wave-number modulus κ_C , *i.e.* independent of the horizontal size of the circulation cells.

4.4. Choice of eddy diffusivities of momentum and heat

It remains to specify the form of the eddy diffusivities of momentum and heat, $\nu_T(z)$ and $\alpha_T(z)$. From micrometeorological experiments, the following empirical expressions have been proposed (Arya 2001, §11.2; *cf.* also Lykossov 2001, §3.2, and Johansson *et al.* 2001)

$$\begin{aligned}\nu_T(z, L_\theta) &\cong \kappa U^* z \varphi_\nu(z/L_\theta), \\ \alpha_T(z, L_\theta) &\cong \kappa U^* z \varphi_\alpha(z/L_\theta),\end{aligned}$$

with similarity functions

$$\begin{aligned}\varphi_\alpha = \varphi_\nu^2 &= (1 - 15z/L_\theta)^{-1/2}, & L_\theta < 0, \\ \varphi_\alpha = \varphi_\nu &= 1 + 5z/L_\theta, & L_\theta > 0,\end{aligned}$$

where the parameter $L_\theta < 0$ applies to unstable conditions, and $L_\theta > 0$ to stable conditions.

However, in view of the uncertainties in the measurements, and because of the singular character of the wind- and temperature profiles at the surface $z = 0$, we take here simply $\alpha_T(z) \equiv \nu_T(z)$. Besides, in accordance with Part 1, expression 30, it is assumed that close to the surface, $0 \leq z \leq z_v$, where the logarithmic velocity profile is not valid, the eddy viscosity is small, and can be represented by a constant value $\nu_s \cong \{\nu + \kappa |U^*| z_{0s}\} f_D(z_v)$; ν is the kinematic viscosity of air, and $f_D(z) \leq 1$, $f_D(z_v) = 1$, a damping function. For $z_v \leq z \leq h$, a profile is chosen as:

$$\nu_T(z) = \{\nu + \kappa |U^*| (z - d)\} f_D(z), \quad (18)$$

with $d = z_v - z_{0s}$.

Thus, the *displacement height* d and the *roughness parameter* z_{0s} should be regarded as parameters in the variational problem (6). To facilitate the analysis, we take as damping function $f_D(z) \equiv 1$; then, integrating (3) and (4),

$$\Theta^*/|U^*| \cong (\Theta_z - \Theta_0) / |U_z - U_0|, \quad (19)$$

where U_0 is the surface current (usually neglected), and Θ_0 is the surface temperature.

5. Dependence of wave growth on Richardson number

As a measure of atmospheric stability due to air-sea temperature differences, a *Richardson number* Ri is defined as (appendix E):

$$Ri \cong 4\kappa / (\pi A_{S\max}) \beta_T (\Theta_z - \Theta_0) gh / |U^* U_z|, \quad (20)$$

where

$\kappa \cong 0.4$ denotes the von Kármán constant;

$A_{S\max} \cong 2.32$ a model-dependent constant;

$\beta_T \cong 0.0033 \text{ (T}^{-1}\text{)}$ the coefficient of thermal expansion;

$\Theta_z - \Theta_0$ the air-sea temperature difference;

g the acceleration of gravity;

h the height of the atmospheric boundary layer;

U^* the *friction velocity* of the wind;

U_z the wind speed at height z .

The growth rate parameter C_β (defined in Part 1, equation (34)) becomes, in terms of Ri ,

$$C_\beta = C_{\beta 0} (1 - Ri/2)^2. \quad (21)$$

Thus, in unstable conditions ($Ri < 0$) wave growth is enhanced whereas in stable conditions ($Ri > 0$) it is reduced (cf. Young 1998); the expression is nearly linear in Ri for small values, $|Ri| < 1/2$. Note that in the last case, $Ri < 2$; otherwise, wave growth is prevented due to stable stratification.

With the estimate $h \cong U^* / (\alpha_0 f_C)$, (cf. Donelan 1990, §3B; Part 1, equation (11)), the Richardson number (20) becomes:

$$Ri \cong 4\kappa / (\pi A_{S\max}) \beta_T (\Theta_z - \Theta_0) g / (\alpha_0 f_C U_z). \quad (22)$$

Some values of Ri and the corresponding relative change in the growth rate parameter $C_\beta / C_{\beta 0}$, for air-sea temperature differences of $\pm 1^\circ$, are given in table 1, showing a significant influence.

$U_z \text{ (m / s)}$	5	10	15	20	25	30
$ Ri $	1.03	0.52	0.34	0.26	0.21	0.17
$C_\beta / C_{\beta 0} (Ri < 0)$	2.30	1.58	1.37	1.27	1.22	1.18
$C_\beta / C_{\beta 0} (Ri > 0)$	0.24	0.55	0.69	0.76	0.80	0.84

Table 1. Richardson number and relative change in growth rate, for $\Theta_z - \Theta_0 = \pm 1^\circ$

Note that these results depend on the approximate value of the parameter $A_{S \max}$ in the expression for Ri , as given in appendix E; this value is presumably somewhat underestimated, and consequently the effect on growth rate overestimated. However, only pure ‘wind input into waves’ is involved in the expression (21) for the growth rate; nonlinear wave-wave interactions and wave dissipation are not considered here. Therefore, the results of table 1 are not directly comparable with the measuring-data of Young (1998); the ‘bulk Richardson number’, applied by Young as an alternative indicator of atmospheric stability, is different from (20).

6. Some model properties. Effects due to shallow water and swell

In order to explain influences of physical processes as shoaling and swell, two model types will be discerned in this section:

- an analytical model, where mean wind and waves (including swell) have the same direction, under neutrally stable conditions;
- a numerical model, dependent on the directional wave spectrum, in the presence of swell and thermal stratification.

6.1. The analytical model

Consider the special case that mean wind and waves are aligned along the x -axis, *i.e.* $q = 0$.

Under neutral stability conditions, the analytical model (which is similar to the simple model (38) of Part 1) is given by

$$\kappa U_z / U^* \cong 1 + d/z_{0s} + \ln [(z-d)/z_{0s}] , \quad (23a)$$

$$(1 - G_m) / (2\kappa k_m z_{0s}) \cong c_m / U^* , \quad (23b)$$

with *shape factor*

$$G_m \equiv \sum_j a_j^2 \exp[-2k_j(d + z_{0s})] , \quad (23c)$$

where a_j the (dimensionless) weight of the spectral component with wave number k_j , normalized by $\sum_j a_j^2 = 1$, mean phase speed $c_m = \varpi_m / k_m$, and mean frequency $\varpi_m \equiv \sum_j a_j^2 \varpi_j$. The ratio c_m / U^* is a measure of the *wave age*. Note that G_m mainly depends on the high-frequency part of the energy density spectrum $a_j^2(k_j)$, and $0 < G_m < 1$. From (23b), the friction velocity U^* can be eliminated, resulting in an equation for the roughness parameter z_{0s} , which can be solved by the method of successive substitution. The drag coefficient is now given by $C_{Dz} \equiv [U^* / U_z]^2$; it turns out that C_{Dz} , as a function of the displacement height $d \cong \gamma_d H_s$, attains a maximum, consistent with the *principle of maximum energy transfer* (*cf.* Part 1, table 2). As such, the model (23) contains no adjustable parameters.

In *shallow water*, the effect of shoaling may generally cause an increase of roughness: according to linear wave theory, in the absence of currents, shoaling waves become steeper, while the mean frequency ω_m remains sensibly constant; the factor $(1 - G_m)$ in (23b) then increases with steepness $k_m d$, resulting in enhanced roughness.

The effect of *swell* can be explained by the same mechanism: a following swell entering the wind wave field reduces the effective steepness, and thereby the roughness and the net growth of the wind waves, whereas an opposing swell enhances this growth, in agreement with laboratory and field observations (*cf.* van den Boogaard *et al.* 1991, p.53). Several other physical mechanisms have been proposed to account for this effect: Balk (1996) showed that a train of long waves can suppress a short-wave field merely by means of four-wave resonance interactions; Booij *et al.* (2002) applied some relatively simple modifications in the formulation for the dissipation ('white-capping') and generation of wind waves, to improve the performance of the third-generation wave model SWAN. Note that weak winds over swell may even show upward momentum transport (*cf.* Grachev and Fairall 2001).

6.1.1. Comparison with the Kitaigorodskii roughness model

Kitaigorodskii (1970) considers in the first instance the propagation of a simple harmonic wave in a coordinate system moving with the phase speed c of the wave; the velocity profile U_z , applying to the atmospheric boundary layer, is then given by the logarithmic wind profile

$$\kappa(U_z - c)/U^* \cong \ln(z/a) , \quad (24a)$$

wherein a a measure is for the amplitude of the wave; now (24a) can be written as

$$\kappa U_z / U^* \cong \ln(z/z_0) , \quad (24b)$$

with roughness parameter

$$z_0 = a \exp[-\kappa c / U^*] . \quad (24c)$$

For a *wave spectrum* with energy density $S(k)$, this can be generalized to

$$z_0^2 \cong C_K^{-2} \int_0^\infty S(k) \exp[-2\kappa c(k)/U^*] dk , \quad (24d)$$

wherein C_K denotes an empirical constant (*cf.* also Donelan 1990, §4, for further discussion on a simplified formula and comparison of results with field data).

It follows easily by inspection, that in the limit of a simple harmonic wave with infinitesimal amplitude $a \rightarrow 0$, the models (23) and (24) become identical, when the roughness z_{0s} in (23) is taken equal to the amplitude a in (24)! This property makes a comparison between both models in case of a *realistic* wave field very interesting (in that case, knowledge is required of the wave number spectrum, notably the high-wave number part).

6.1.2. Comparison with observations

The RASEX (Risø Air-Sea Exchange) field experiment was carried out in rather shallow water (3m to 4m), at an off-shore fetch-limited site in the Baltic sea at Vindeby, Denmark in 1994 (for details, see Johnson *et al.* 1998; Taylor and Yelland 2001). A few cases are selected here from table 1 in Johnson *et al.* (1998), where locally wind-generated waves were considered in neutrally stratified situations, with wind and waves in nearly the same direction and rough turbulent-flow conditions at the air-sea interface; the measured drag coefficients are in the range $1 \cdot 10^{-3}$ to $2 \cdot 10^{-3}$.

In table 2 below, some typical values of the measured drag coefficient are presented, together with results of the roughness length formula of Taylor and Yelland (2001), and with results of the model (23), using a Wallops-type spectrum with high-frequency tail ω^{-4} .

U_{10n} (m / s)	4.14	6.41	8.89	10.33	12.72	15.14	16.35
Measured (RASEX)	1.7	1.3	1.5	1.5	1.5	1.8	1.8
Taylor and Yelland	1.1	1.2	1.4	1.5	1.6	1.7	1.8
Present model (23)	0.03	0.3	0.6	1.2	2.1	3.3	3.9

Table 2. Comparison of some values of the drag coefficient C_{Dn} in units of 10^{-3}

Taylor and Yelland (2001) used, together with HEXOS (Meetpost Noordwijk) and AD96 (Lake Ontario) data, only RASEX data where $U_{10n} > 10$ m/s to determine the coefficients in their roughness length formula by regression analysis.

Although the measurements show a large scatter in roughness especially in case of weaker wind speeds, $U_{10} < 10$ m/s, the model (23) predicts in that case far too low values of the drag coefficient; for $U_{10} > 13$ m/s, the model overestimates the drag coefficient. In these conditions, the simple model (23) is not merely applicable, even considering the sensitive dependence of the surface drag on spectral shape; however, it should be stressed that the model contains no adjustable parameters.

6.2. The numerical model

The analytical model is essentially based on the approximation $\underline{P}_S \cong 0$, *i.e.* the average-over-height of the *pseudo-momentum* is supposed to be zero; as appears from the foregoing, this approximation is generally not justified. According to the analysis in appendix F, correction terms emerge in the right-hand side of equation (23b), resulting in enhanced roughness z_{0s} . However, the precise effect of these terms on the surface drag is not easy to analyse; the sensitivity of the roughness to the mean wind shear (*i.e.* to the profile of the wave-induced wind stress $\langle wu \rangle$, *cf.* Part 1, figure 1) may be considerable, and an accurate numerical approach is necessary.

The wave-induced wind stress *c.q.* heat flux (16) is proportional to the solution $m_0(z)$ of equation (E3):

$$\nu_T \partial_z^2 m_0 = [G_\Theta(z) - qH_\Theta(z)] / \sqrt{1+q^2} \quad , \quad (25)$$

which has to be found generally by numerical means. The right-hand side of (25) depends on the directional wave spectrum, as well as on the mean wind shear $\partial U / \partial z$, and the orientation q , between the directions of shear flow and pseudo-momentum (*cf.* Cox 1997). With the mean wind shear given by (3), and boundary conditions $m_0 = 0$ at $z = 0$ and $z = h$, the equation is linear in $m_0(z)$, with coefficients still depending on the parameters d and z_{0s} .

Thus, invoking the principle of maximum energy transfer, the problem amounts to solving (25) for $m_0(z)$ and obtaining the maximum value of dE/dt in (E8) by variation of the parameters d and z_{0s} ; the friction velocity U^* then follows from integrating the mean wind shear $\partial_z U$ in (3) to the wind speed U_{zM} measured at a given height z_M .

The numerical model (25) should be used to test the validity of the analytical model (23), in particular:

- the approximation $\underline{P}_S \cong 0$, *i.e.* the average-over-height of the *pseudo-momentum* is zero;
- the sensitivity to mean wind shear near the sea surface (effect of eddy viscosity model);
- the sensitivity to spectral shape (effect of swell *c.q.* high-frequency spectral tail);
- the assumption that mean wind and waves are aligned (effect of wave refraction);
- the ‘constant stress layer’ assumption.

As an alternative to the simple eddy viscosity model (18), a (k - ϵ) turbulence model may be suitable, *cf.* Araujo *et al.* (2001). A new analytical model for the high-frequency tail of the wind-wave spectrum is proposed by Hara and Belcher (2002).

7. Concluding remarks

In the present work, the effect of atmospheric stability due to air-sea temperature differences $\Delta\Theta$ on wave growth by wind is investigated. For small values of the *Richardson number* (20) involved, the change in growth rate is found to be proportional to the height h of the convective boundary layer, inversely proportional to the wind speed U_z and the friction velocity U^* , and is enhanced / reduced in unstable / stable conditions: in stormy weather, the relative change in growth rate per degree $\Delta\Theta$ is estimated to be 20 to 30 % (*cf.* table 1).

While the present *analytical* model is asymptotically equivalent to the Kitaigorodskii roughness model, its performance in calm *c.q.* stormy weather (*cf.* table 2) and its sensitivity to spectral shape *c.q.* mean wind shear near the sea surface need further study; the proposed *numerical* model may serve this purpose, and more in general the aim to validate the CL-theory, as applied here to the problem of momentum and heat transfer between air and sea.

Comparing model results with measuring-data, one should taken into account that generally:

- mean wind and waves have different directions, especially in shallow water;
- the shape of the directional spectrum is of importance;
- at lower wind speeds, surface (tidal) currents exert influence;
- the wind direction depends on height (wind veering: Coriolis effect).

In order to evaluate the effect of the various assumptions made in the underlying theory, comparison with (laboratory and field) observations of wind and waves as well as with numerical simulations (DNS, LES) is necessary.

Available field measurements in the Netherlands have been presented by Andorka Gal (1996) for the coastal area of Petten, and by Bottema (2002) for the lake IJsselmeer area.

Numerical simulations of turbulent flow over waves have been performed by Phillips *et al.* (1996), Li *et al.* (2000) and Sullivan and McWilliams (2002). Khanna and Brasseur (1997) reported a detailed analysis of the Monin-Obukhov similarity from high-resolution LES predictions.

Acknowledgement

The results presented in table 2 were calculated by M. Zijlema.

Appendix A. The isothermal boundary condition $\theta = 0$

At *zeroth* order, we have

$$\partial_z w_0 = 0, \quad (\text{A1a})$$

$$w_0 \partial_z U_\pi = \partial_z (v_T \partial_z u_0), \quad (\text{A1b})$$

$$w_0 \partial_z V_\pi = \partial_z (v_T \partial_z v_0), \quad (\text{A1c})$$

$$\partial_z p_0 = 2 \partial_z (v_T \partial_z w_0) + P_S \partial_z u_0 + Q_S \partial_z v_0 + \beta_T g \theta_0, \quad (\text{A1d})$$

$$w_0 \partial_z \Theta = \partial_z (\alpha_T \partial_z \theta_0), \quad (\text{A1e})$$

with $\partial_z \equiv \partial/\partial z$.

Together with the boundary conditions (9), we obtain from (A1a): $w_0 \equiv 0$; from (A1b,c): u_0, v_0 are constants, generally $\neq 0$; from (A1d,e): $\theta_0 \equiv 0$ (because of the boundary condition $\theta = 0$, and $\alpha_T > 0$ on $0 \leq z \leq h$), and p_0 constant $\neq 0$.

At *first* order:

$$i(ku_0 + lv_0) + \partial_z w_1 = 0, \quad (\text{A2a})$$

$$\sigma_1 u_0 + i(kU_\pi + lV_\pi) u_0 + w_1 \partial_z U_\pi + ik p_0 = \partial_z (v_T \partial_z u_1) - Q_S i(lu_0 - kv_0), \quad (\text{A2b})$$

$$\sigma_1 v_0 + i(kU_\pi + lV_\pi) v_0 + w_1 \partial_z V_\pi + il p_0 = \partial_z (v_T \partial_z v_1) + P_S i(lu_0 - kv_0), \quad (\text{A2c})$$

$$\partial_z p_1 = 2 \partial_z (v_T \partial_z w_1) + P_S \partial_z u_1 + Q_S \partial_z v_1 + \beta_T g \theta_1, \quad (\text{A2d})$$

$$w_1 \partial_z \Theta = \partial_z (\alpha_T \partial_z \theta_1). \quad (\text{A2e})$$

Integrating the continuity equation (A2a) gives, in view of the boundary conditions (9), $ku_0 + lv_0 = 0$, and so $w_1 \equiv 0$; likewise, from (A2e): $\theta_1 \equiv 0$. Averaging the momentum equations over height, it is found that $p_0 = (l \underline{P}_S - k \underline{Q}_S)(lu_0 - kv_0) / (k^2 + l^2)$, where $\underline{P}_S, \underline{Q}_S$ denote averages over height h .

At *second* order:

$$i(ku_1 + lv_1) + \partial_z w_2 = 0. \quad (\text{A3})$$

Elimination of u_1, v_1 from this equation and the *first* order momentum equations yields:

$$\partial_z (v_T \partial_z^2 w_2) = [l(\underline{P}_S - P_S) - k(\underline{Q}_S - Q_S)](lu_0 - kv_0), \quad (\text{A4})$$

$$\text{and} \quad w_2 \partial_z \Theta = \partial_z (\alpha_T \partial_z \theta_2), \quad (\text{A5})$$

with boundary conditions: $w_2 = 0, \partial_z^2 w_2 = 0$, and $\theta_2 = 0$ at $z = 0$ and $z = h$.

Appendix B. The boundary condition $\partial\theta/\partial z = 0$

At *zeroth* order, we have

$$\partial_z w_0 = 0, \quad (\text{B1a})$$

$$w_0 \partial_z U_\pi = \partial_z (v_T \partial_z u_0), \quad (\text{B1b})$$

$$w_0 \partial_z V_\pi = \partial_z (v_T \partial_z v_0), \quad (\text{B1c})$$

$$\partial_z p_0 = 2 \partial_z (v_T \partial_z w_0) + P_S \partial_z u_0 + Q_S \partial_z v_0 + \beta_T g \theta_0, \quad (\text{B1d})$$

$$w_0 \partial_z \Theta = \partial_z (\alpha_T \partial_z \theta_0). \quad (\text{B1e})$$

In view of the boundary conditions, we obtain: $w_0 \equiv 0$; u_0 , v_0 and θ_0 are constants, generally $\neq 0$; and $\partial_z p_0 = \beta_T g \theta_0$ constant $\neq 0$, so $p_0 = \underline{p}_0 + \beta_T \theta_0 g (z - h/2)$.

At *first* order:

$$i(ku_0 + lv_0) + \partial_z w_1 = 0, \quad (\text{B2a})$$

$$\sigma_1 u_0 + i(kU_\pi + lV_\pi) u_0 + w_1 \partial_z U_\pi + ik p_0 = \partial_z (v_T \partial_z u_1) - Q_S i(lu_0 - kv_0), \quad (\text{B2b})$$

$$\sigma_1 v_0 + i(kU_\pi + lV_\pi) v_0 + w_1 \partial_z V_\pi + il p_0 = \partial_z (v_T \partial_z v_1) + P_S i(lu_0 - kv_0), \quad (\text{B2c})$$

$$\partial_z p_1 = 2 \partial_z (v_T \partial_z w_1) + P_S \partial_z u_1 + Q_S \partial_z v_1 + \beta_T g \theta_1, \quad (\text{B2d})$$

$$\sigma_1 \theta_0 + i(kU + lV) \theta_0 + w_1 \partial_z \Theta = \partial_z (\alpha_T \partial_z \theta_1). \quad (\text{B2e})$$

Integrating the continuity equation (B2a) gives: $ku_0 + lv_0 = 0$, and so $w_1 \equiv 0$; eliminating p_0 from (B2b,c) and averaging over height, it is found that

$$\sigma_1 = -i [k(\underline{U} + \underline{U}_S) + l(\underline{V} + \underline{V}_S)]. \quad (\text{B3})$$

Now, the pseudo-momentum and the Stokes drift are $\mathcal{O}(a^2)$, with wave amplitude $a = \mathcal{O}(\varepsilon)$, so in the present order of approximation we have

$$U_\pi \equiv \underline{U} + \mathcal{O}(\varepsilon^2), \quad \sigma_1 = -i (k\underline{U} + l\underline{V}) + \mathcal{O}(\varepsilon^2). \quad (\text{B4})$$

Using $ku_0 + lv_0 = 0$, and averaging the momentum equations (B2b,c) over height,

$$\underline{p}_0 = (l \underline{P}_S - k \underline{Q}_S)(lu_0 - kv_0) / (k^2 + l^2). \quad (\text{B5})$$

At *second* order:

$$i(ku_1 + lv_1) + \partial_z w_2 = 0 . \quad (\text{B6a})$$

$$\sigma_2 u_0 + w_2 \partial_z U_\pi + ik p_1 = \partial_z (v_T \partial_z u_2) - Q_S i(lu_1 - kv_1) - v_T (k^2 + l^2) u_0 , \quad (\text{B6b})$$

$$\sigma_2 v_0 + w_2 \partial_z V_\pi + il p_1 = \partial_z (v_T \partial_z v_2) + P_S i(lu_1 - kv_1) - v_T (k^2 + l^2) v_0 , \quad (\text{B6c})$$

$$\partial_z p_2 = 2 \partial_z (v_T \partial_z w_2) + i v_T \partial_z (ku_1 + lv_1) + P_S \partial_z u_2 + Q_S \partial_z v_2 + \beta_T g \theta_2 , \quad (\text{B6d})$$

$$\sigma_2 \theta_0 + w_2 \partial_z \Theta = \partial_z (\alpha_T \partial_z \theta_2) - \alpha_T (k^2 + l^2) \theta_0 . \quad (\text{B6e})$$

Elimination of u_1, v_1 from the continuity equation (B6a) and the first order momentum equations (B2b,c) yields:

$$\partial_z (v_T \partial_z^2 w_2) = [l(\underline{P}_S - P_S) - k(\underline{Q}_S - Q_S)] (lu_0 - kv_0) + (k^2 + l^2) \beta_T \theta_0 g (z - h/2) . \quad (\text{B7})$$

Averaging (B6e) over height,

$$[\sigma_2 + (k^2 + l^2) h^{-1} \int_0^h dz \alpha_T] \theta_0 = - h^{-1} \int_0^h dz w_2 \partial_z \Theta , \quad (\text{B8})$$

it remains to evaluate the *growth rate* σ_2 : eliminating p_1 from (B6b,c) and averaging over height, we obtain

$$\begin{aligned} \sigma_2 = & - (k^2 + l^2) h^{-1} \int_0^h dz v_T \\ & - h^{-1} \int_0^h dz [w_2 \partial_z (lU - kV) - i(kP_S + lQ_S)(lu_1 - kv_1)] / (lu_0 - kv_0) . \end{aligned} \quad (\text{B9})$$

When wind and waves are aligned (*i.e.* shear flow and pseudo-momentum in the same direction) it follows that $kP_S + lQ_S \equiv 0$; in any case, $(P_S, Q_S) = \mathcal{O}(\epsilon^2)$, and we may neglect the corresponding term in (B9). Then (B8) becomes

$$\int_0^h dz [(k^2 + l^2)(\alpha_T - v_T) - w_2 \partial_z (lU - kV)/(lu_0 - kv_0)] \theta_0 = - \int_0^h dz w_2 \partial_z \Theta . \quad (\text{B10})$$

Appendix C. Coefficients of momentum- and heat-fluxes

From $lu_0 - kv_0 = \kappa_C A_0$ and $ku_0 + lv_0 = 0$, with $\kappa_C = \sqrt{(k^2 + l^2)}$, and $q = k/l$ denoting the orientation of the critical rolls, we have

$$u_0 = lA_0/\kappa_C, \quad v_0 = -q lA_0/\kappa_C, \quad w_2(z) = \kappa_C^2 A_0 m_0(z), \quad \text{and} \quad \theta_0 = A_0 \theta_m. \quad (\text{C1})$$

Upon substituting the real part of the solution (10) into (3), (4) and subsequently into (5), and neglecting in the final expressions terms of $\mathcal{O}(\varepsilon^2)$, we obtain

$$\int_0^h dz \{ \frac{1}{2} v_T \langle 2\mathbf{d}:2\mathbf{d} \rangle \} \cong \frac{1}{2} \kappa_C^2 A_0^2 \int_0^h dz v_T, \quad (\text{C2})$$

$$\begin{aligned} \int_0^h dz \{ \langle w\mathbf{u} \rangle \cdot \partial(\mathbf{U} + \mathbf{U}_S)/\partial z \} &\cong \frac{1}{2} \kappa_C^2 A_0^2 \int_0^h dz m_0(z) [Z_x - qZ_y]/\sqrt{(1+q^2)} + \\ &\quad \frac{1}{4} \kappa_C^4 A_0^4 \int_0^h dz m_0^2(z) / v_T, \end{aligned} \quad (\text{C3})$$

$$\int_0^h dz \{ \beta_T g \langle w\theta \rangle \} \cong \frac{1}{2} \kappa_C^2 A_0^2 g \beta_T \theta_m \int_0^h dz m_0(z), \quad (\text{C4})$$

where $\mathbf{Z} \equiv (Z_x, Z_y) \equiv |\mathbf{U}^*| \mathbf{U}^*/v_T + \partial \mathbf{U}_S/\partial z$.

Then, the *equilibrium* amplitude A_0 of the governing *Landau-Stuart* equation is:

$$\kappa_C^2 A_0^2 = (\alpha - \beta)/\gamma, \quad (\text{C5})$$

with coefficients α , β and γ given by

$$\alpha = -2 \int_0^h dz m_0(z) \{ (Z_x - qZ_y)/\sqrt{(1+q^2)} - g\beta_T \theta_m \}, \quad (\text{C6a})$$

$$\beta = 2 \int_0^h dz v_T, \quad \gamma = \int_0^h dz m_0^2(z) / v_T, \quad (\text{C6b,c})$$

where the *Landau* constant $\gamma > 0$ allows supercritical behaviour of the solution, and the existence of a non-trivial equilibrium-flow state for the profile $m_0(z)$ and the constant θ_m , when $\alpha > \beta$.

Note that the coefficient α depends explicitly on the orientation q of the critical rolls.

Appendix D. Evaluation of the temperature disturbance θ_m

To evaluate θ_m from (15b), we need to specify the (empirical) forms of the eddy diffusivities of momentum and heat, $\nu_T(z)$ and $\alpha_T(z)$.

According to §4.4, assuming that $\nu_T \equiv \alpha_T$, then

$$\theta_m \int_0^h dz \, m_0 \partial_z (U - qV) / \sqrt{(1+q^2)} = \int_0^h dz \, m_0 \partial_z \Theta, \quad (\text{D1})$$

or, with (3), (4), (16) and (17), using $V^* = -q U^*$,

$$\theta_m \int_0^h dz \, m_0 [\langle wu \rangle + |U^*| U^*] / \nu_T = \int_0^h dz \, m_0 [\langle wu \rangle \theta_m + |U^*| \Theta^* / \sqrt{(1+q^2)}] / \nu_T. \quad (\text{D2})$$

The solution of this equation is given by

$$\theta_m / \sqrt{(1+q^2)} = \Theta^* / (U^* - qV^*). \quad (\text{D3})$$

In view of $V^* = -q U^*$, we have then simply

$$\theta_m = \Theta^* / |U^*|. \quad (\text{D4})$$

Appendix E. Definition of Richardson number. Approximate solution $m_0(z)$ for $q = 0$

The pseudo-momentum \mathbf{P}_S is defined by

$$\mathbf{P}_S(z) \equiv (P_S, Q_S) = \partial_z \mathbf{G}_S \equiv \partial_z (G_S, H_S), \quad (\text{E1})$$

with primitive function

$$\mathbf{G}_S(z) \equiv \frac{1}{2} a^2 \sum_j a_j^2 [-\exp(-2k_j z) c_j \mathbf{k}_j + k_j \int_z^h dz' \exp(-2k_j z') \partial U / \partial z']. \quad (\text{E2})$$

Herein, a is a wave amplitude, related to the spectral wave energy E by $E = \frac{1}{2} \rho_w g a^2$, a_j the dimensionless weight of the spectral component with wave number \mathbf{k}_j and phase velocity c_j , normalized by $\sum_j a_j^2 = 1$, $k_j = |\mathbf{k}_j|$, and $\partial U / \partial z$ denotes the mean wind shear.

Integrating (15a) once, the equation for $m_0(z)$ can be written in the form

$$v_T \partial_z^2 m_0 = [G_\Theta(z) - q H_\Theta(z)] / \sqrt{1+q^2}, \quad (\text{E3})$$

where

$$G_\Theta(z) = (z/h) G_S(h) + (1-z/h) G_S(0) - G_S(z) + \frac{1}{2} \beta_T \Theta^* g z(z-h) / (U^* - qV^*), \quad (\text{E4a})$$

$$H_\Theta(z) = (z/h) H_S(h) + (1-z/h) H_S(0) - H_S(z) - q \frac{1}{2} \beta_T \Theta^* g z(z-h) / (U^* - qV^*), \quad (\text{E4b})$$

with

$$G_\Theta(h) = G_\Theta(0) = H_\Theta(h) = H_\Theta(0) = 0, \text{ and boundary conditions } m_0 = 0 \text{ at } z = 0 \text{ and } z = h.$$

Substituting (3) into (6) and neglecting the $\mathcal{O}(a^2)$ Stokes-drift term results in:

$$dE/dt \equiv - \int_0^h dz \rho_a \{ \langle wu \rangle \cdot (\langle wu \rangle + |\mathbf{U}^*| \mathbf{U}^*) / v_T - g \beta_T \langle w\theta \rangle \}, \quad (\text{E5})$$

which, being a quadratic expression in $\langle wu \rangle$, turns out to have a maximum value.

Defining the dimensionless coefficients (from appendix C, neglecting the $\partial_z \mathbf{U}_S$ - term):

$$\alpha_S = \alpha / (2 |\mathbf{U}^*| h^2); \quad \beta_S = \beta / (2 |\mathbf{U}^*| h^2); \quad \gamma_S = \gamma |\mathbf{U}^*| / h^4; \quad (\text{E6a})$$

$$\Gamma_S = \frac{1}{2} [(\alpha - \beta) / \gamma] h^2 / |\mathbf{U}^*|^2, \quad (\text{E6b})$$

we have $\Gamma_S = (\alpha_S - \beta_S) / \gamma_S$.

Upon substituting these expressions into (E5), using (16), we obtain

$$dE/dt \cong \rho_a |U^*|^3 \beta_S (\alpha_S - \beta_S) / \gamma_S , \quad (E7)$$

where the coefficients still depend on $m_0(z)$, and in turn via v_T also on the parameters d and z_{0s} (note that the coefficient α_S depends explicitly on the orientation q of the critical rolls). Consequently, dE/dt can be conceived as a functional of $m_0(z)$, and employing the concept of variational, or functional derivative (*cf.* Dingemans 1997, §1.5.2), it is easily shown that dE/dt attains a maximum when $\alpha_S = 2\beta_S$, and

$$dE/dt|_{\max} \cong \rho_a |U^*|^3 \beta_S^2 / \gamma_S = \rho_a |U^*|^3 \alpha_S^2 / (4\gamma_S) , \quad (E8)$$

Thus, invoking the *principle of maximum energy transfer*, the problem amounts to solving (E3) for $m_0(z)$ and obtaining the maximum value of dE/dt in (E8) by variation of the parameters d and z_{0s} ; the friction velocity U^* then follows from integrating the mean wind shear $\partial_z U$ in (3) to the wind speed U_{zM} measured at a given height z_M .

As a measure of atmospheric stability due to air-sea temperature differences, a *Richardson number* Ri is defined as follows:

$$\alpha_S = \alpha_{S0} (1 - Ri/2) , \quad (E9)$$

where α_{S0} is equal to α_S without temperature effect (*i.e.* $\theta_m = 0$). In order to obtain a workable expression for Ri , an estimate of the integral $\int_0^h dz m_0(z)$ is needed.

The solution $m_0(z)$ of equation (E3) can be written in the form

$$m_0(z) = \sum_n m_{0n} \sin(n\pi z/h) , \quad (E10)$$

where the boundary conditions: $m_0 = 0$ and $\partial_z^2 m_0 = 0$, at $z = 0$ and $z = h$, are satisfied automatically. The coefficients m_{0n} can be found numerically by standard methods, *e.g.* collocation. Here, an approximate solution will be given in the form (for $q = 0$, *cf.* Part 1):

$$m_0(z) \cong m_{01} \{ \sin(\pi z/h) + b \sin(2\pi z/h) \} , \quad (E11)$$

in order to estimate the value of the integral $\int_0^h dz m_0(z)$.

From the analysis in Part 1 (appendix E, with $f_D \equiv 1$) we arrive at

$$m_{01} / h^2 \cong -\kappa^2 / A_S , \quad (E12)$$

where

$$A_S = A_{S \max} \cong C_1 + b_{\max} C_2 , \quad b = b_{\max} \cong 0.32 , \quad (E13a)$$

$$C_1 = \int_0^\pi dz \sin z / z \equiv \text{Si}(\pi) = 1.8519 , \quad C_2 = \int_0^{2\pi} dz \sin z / z \equiv \text{Si}(2\pi) = 1.4182 , \quad (E13b)$$

(For the definition of the Sine Integral, see Abramowitz and Stegun 1968, §5.2).

With the approximation (E11) the Richardson number Ri can be written in the form

$$Ri \cong 4\kappa / (\pi A_{S \max}) \beta_T \Theta^* gh / |\mathbf{U}^*|^2 . \quad (E14)$$

From the expression (19) for Θ^* , with $\mathbf{U}_0 \cong 0$, we obtain finally

$$Ri \cong 4\kappa / (\pi A_{S \max}) \beta_T (\Theta_z - \Theta_0) gh / |\mathbf{U}^* \mathbf{U}_z| . \quad (E15)$$

The value of $A_{S \max}$ follows from (E13): $A_{S \max} \cong 2.32$.

Appendix F. Estimation of the mean value of the pseudo-momentum P_S

In Part 1, a simple model was derived for the wave-induced wind stress, based on the approximation $\underline{P}_S \cong 0$, *i.e.* the average-over-height value of the *pseudo-momentum* was supposed to be zero. Here, an alternative estimation of \underline{P}_S will be given: according to (E1) and (E2), the pseudo-momentum P_S decays exponentially with height z , so $P_S(h) \cong 0$ and $G_S(h) \cong 0$ as $2k_m h \gg 1$.

Then, from (15a, $q = 0$; $z = 0$) we have:

$$\underline{P}_S = P_S(0) + \partial_z(v_T \partial_z^2 m_0)|_0 + \frac{1}{2} g h \beta_T \theta_m, \quad (\text{F1a})$$

and:

$$\underline{P}_S \cong -G_S(0)/h. \quad (\text{F1b})$$

The expression (C5) from Part 1 is given by

$$G_S(0) \cong \frac{1}{2} a^2 [-c_m k_m + U^*(1 - G_m)/(2\kappa z_{0s})], \quad (\text{F2})$$

with *shape factor*

$$G_m \equiv \sum_j a_j^2 \exp[-2k_j(d + z_{0s})]. \quad (\text{F3})$$

From (E1) and (E2),

$$P_S(0) \cong a^2 \{ \sum_j a_j^2 c_j k_j^2 - \frac{1}{2} k_m \partial U / \partial z |_0 \}. \quad (\text{F4})$$

Under neutral stability conditions ($\theta_m = 0$), using (E11) and (E12), we obtain, with $v_T(0) \cong \kappa U^* z_{0s}$,

$$\underline{P}_S \cong a^2 \{ \sum_j a_j^2 c_j k_j^2 - k_m U^* / (2\kappa z_{0s}) \} + \frac{1}{2} \lambda_0 U^* z_{0s} / h, \quad (\text{F5})$$

where $\lambda_0 = 2(1+8b)(\kappa\pi)^3/A_S \cong 6.09$; further, assuming the frequency spectrum sufficiently narrow, $\sum_j a_j^2 c_j k_j^2 \cong c_m k_m^2$, we obtain

$$(1 - G_m) / (2\kappa k_m z_{0s}) \cong c_m / U^* - \lambda_0 k_m z_{0s} / (k_m a)^2 + (1 - 2\kappa k_m z_{0s} c_m / U^*) h / (\kappa z_{0s}), \quad (\text{F6})$$

wherein some correction terms emerge, in comparison with equation (23b). In order to eliminate z_{0s} from (F6), let $x = 2\kappa k_m z_{0s} c_m / U^*$; $p = \lambda_0 / [2\kappa(k_m a c_m / U^*)^2]$; $q = 2k_m h - 1$; $r = 2k_m h - (1 - G_m)$; then x must satisfy

$$p x^2 + q x - r = 0, \quad (\text{F7})$$

with p, q and $r > 0$.

The quadratic equation (F7) has a solution $x > 0$,

$$x = \frac{1}{2} [\sqrt{(1 + 4pr/q^2)} - 1] q/p . \quad (\text{F8})$$

As $2k_m h \gg 1$, we have $q = r \cong 2k_m h$, and obtain

$$x = \frac{1}{2} [\sqrt{(1 + 4p/q)} - 1] q/p . \quad (\text{F9})$$

Alternatively, U^* can be eliminated from (F6), using the approximation $2k_m h \gg 1$, and the estimate $h \cong U^*/(\alpha_0 f_C)$, to yield an expression equivalent to (F9):

$$U^*/c_m \cong 2\kappa k_m z_{0s} [1 + \lambda_0 \alpha_0 f_C k_m z_{0s} / (2\varpi_m (k_m a)^2)] , \quad (\text{F10})$$

which is comparable with equation (23b). For a North-Sea situation under neutral conditions, the constant $\alpha_0 \cong 12$, and the Coriolis parameter $f_C = 1.15 \times 10^{-4} \text{sec}^{-1}$, cf. Donelan (1990).

It should be noted that due to the neglect of the $(1-G_m)$ -term in (F6), the equivalent expressions (F9) and (F10) become independent of the displacement height d ; as a consequence, in the calculation of the drag coefficient C_{Dn} , d becomes an adjustable parameter, scaled as $d \cong \gamma_d H_s$, with $\gamma_d = \mathcal{O}(1)$. Some results of the calculation are shown in table F1, to be compared with the RASEX-results of table 2 (it turns out that the λ_0 -term in F10 is $\mathcal{O}(10^{-2})$ and can be neglected).

However, these model results depend essentially on the (rough) approximation of the shear term $\partial_z(v_T \partial_z^2 m_0)|_0$ by the λ_0 -term in the expression (F5): being the product of a small factor $v_T(0)$ and a large factor $(\partial_z^3 m_0)|_0$, its value should be tested by an accurate numerical model.

Thus, the model results may be found sensitive to

- the effect of the applied simple eddy viscosity model,
 - the shear of the wave-induced wind stress,
- close to the sea surface.

U_{10n} (m / s)	6.41	10.33	15.14
$\gamma_d = 1.0$	2.3	4.0	6.4
$\gamma_d = 1.4$	1.3	2.6	4.6
$\gamma_d = 2.0$	0.3	1.2	2.6

Table F1. Some values of the drag coefficient C_{Dn} in units of 10^{-3} (model F10)

References

- Abramowitz, M. and Stegun, I.A., eds. 1968
Handbook of Mathematical Functions. Dover Publications, 1046 pp.
- Andorka Gal, J.H. 1996
Verification set Petten. January 1, 1995 - January 10, 1995.
Report RIKZ/OS-96.137x , Rijkswaterstaat/RIKZ, July 1996, 44 pp.
- Araujo, M., Dartus, D., Maurel, Ph. and Masbernat, L. 2001
Langmuir circulations and enhanced turbulence beneath wind-waves.
Ocean Modelling **3**, 109-126.
- Arya, S.P. 2001
Introduction to Micrometeorology. Academic Press, 2nd ed., 415 pp.
- Balk, A.M. 1996
The suppression of short waves by a train of long waves. *J. Fluid Mech.* **315**, 139-150.
- Bejan, A. 2000
Shape and Structure, from Engineering to Nature. Cambridge University Press, 324 pp.
- Bonekamp, H., Komen, G.J., Sterl, A., Janssen, P.A.E.M., Taylor, P.K. and Yelland, M.J. 2002
Statistical comparisons of observed and ECMWF modeled open ocean surface drag.
J. Phys. Oceanogr. **32**(3), 1010-1027.
- Boogaard, H.F.P. van den, Uittenbogaard, R.E. and Gerritsen, H. 1991
The dependence of surface drag on waves. A literature survey.
WL | delft hydraulics, Report Z462, October 1991, 75 pp.
- Booij, N., Holthuijsen, L.H. and Haagsma, IJ. 2002
The effect of swell on the generation and dissipation of wind sea.
In: *Ocean Wave Measurement and Analysis. Proc. WAVES 2001 Conf.*,
Edge, B.L. and Hemsley, J.M. eds., ASCE, Volume One, pp. 501-506.
- Bottema, M. 2002
Rapportage golfmetingen IJsselmeergebied 2000-2001.
Validatie en documentatie meetseizoen 2000-2001.
Werkdocument 2002.063.X, Rijkswaterstaat/RIZA, 8 maart 2002, 94 pp. (in Dutch)
- Busse, F.H. 1978
The optimum theory of turbulence. *Adv. Appl. Mech.* **18**, 77-121.
- Cox, S.M. 1997
Onset of Langmuir circulation when shear flow and Stokes drift are not parallel.
Fluid Dyn. Res. **19**(3), 149-167.
- Cox, S.M. and Leibovich, S. 1993

Langmuir circulations in a surface layer bounded by a strong thermocline.
J. Phys. Oceanogr. **23**(7), 1330-1345.

Csanady, G.T. 2001
Air-Sea Interaction: Laws and Mechanisms. Cambridge University Press, 239 pp.

Dingemans, M.W. 1997
Water wave propagation over uneven bottoms. World Scientific, 967 pp.

Dingemans, M.W. 2001
3D wave-current modelling. Part 2: extension and application to air-sea interaction.
WL | delft hydraulics, Report X251, August 2001, 59 pp.

Doering, C.R. and Constantin, P. 1992
Energy dissipation in shear driven turbulence. *Phys. Rev. Lett.* **69**, 1648-1651.

Donelan, M.A. 1990
Air-sea interaction. In: *The Sea. Ocean Engineering Science*, Vol. **9A**,
Le Méhauté, B. and Hanes, D.M. eds., Wiley-Interscience, pp. 239-292.

Grachev, A.A. and Fairall, C.W. 2001
Upward momentum transfer in the marine boundary layer.
J. Phys. Oceanogr. **31**(7), 1698-1711.

Hara, T. and Belcher, S.E. 2002
Wind forcing in the equilibrium range of wind-wave spectra.
J. Fluid Mech. **470**, 223-245.

Howard, L.N. 1972
Bounds on flow quantities. *Ann. Rev. Fluid Mech.* **4**, 473-494.

Johansson, C., Smedman, A., Höglström, U., Brasseur, J.G. and Khanna, S. 2001
Critical test of the validity of Monin-Obukhov similarity during convective conditions.
J. Atmos. Sci. **58**(12), 1549-1566. (Comments by Andreas, E.L. and Hicks, B.B., and
Reply, *J. Atmos. Sci.* **59**(17), 2605-2614.)

Johnson, H.K., Højstrup, J., Vested, H.J. and Larsen, S.E. 1998
On the dependence of sea surface roughness on wind waves.
J. Phys. Oceanogr. **28**(9), 1702-1716.

Jones, I.S.F. and Toba, Y., eds. 2001
Wind Stress over the Ocean. Cambridge University Press, 336 pp.

Kerswell, R.R. 2002
Upper bounds on general dissipation functionals in turbulent shear flows:
revisiting the ‘efficiency’ functional. *J. Fluid Mech.* **461**, 239-275.

Khanna, S. and Brasseur, J.G. 1997
Analysis of Monin-Obukhov similarity from large-eddy simulation.
J. Fluid Mech. **345**, 251-286.

Kitaigorodskii, S.A. 1970
The physics of air-sea interaction. Israel Program for Scientific Translations,

Jerusalem 1973, 273 pp.

Leibovich, S. 1983

The form and dynamics of Langmuir circulations. *Ann. Rev. Fluid Mech.* **15**, 391-427.

Leibovich, S. and Paolucci, S. 1980

The Langmuir circulation instability as a mixing mechanism in the upper ocean.
J. Phys. Oceanogr. **10**(2), 186-207.

Li, P.Y., Xu, D. and Taylor, P.A. 2000

Numerical modelling of turbulent air flow over water waves.
Boundary-Layer Meteorology **95**(3), 397-425.

Lin, W., Sanford, L.P., Suttles, S.E. and Valigura, R. 2002

Drag coefficients with fetch-limited wind waves.
J. Phys. Oceanogr. **32**(11), 3058-3074.

Lykossov, V.N. 2001

Atmospheric and oceanic boundary layer physics. In: *Wind Stress over the Ocean*.
Jones, I.S.F. and Toba, Y. eds., Cambridge University Press.

Malkus, W.V.R. 1956

Outline of a theory of turbulent shear flow. *J. Fluid Mech.* **1**, 521-539.

Malkus, W.V.R. and Smith, L.M. 1989

Upper bounds on functions of the dissipation rate in turbulent shear flow.
J. Fluid Mech. **208**, 479-507.

McNaughton, K.G. and Brunet, Y. 2002

Townsend's hypothesis, coherent structures and Monin-Obukhov similarity.
Boundary-Layer Meteorology **102**(2), 161-175.

Nicodemus, R., Grossmann, S. and Holthaus, M. 1998

The background flow method.
Part 1. Constructive approach to bounds on energy dissipation. *J. Fluid Mech.* **363**, 281-300.
Part 2. Asymptotic theory of dissipation bounds. *J. Fluid Mech.* **363**, 301-323.

Oberlack, M. 2001

A unified approach for symmetries in plane parallel turbulent shear flows.
J. Fluid Mech. **427**, 299-328.

Phillips, W.R.C., Wu, Z. and Lumley, J.L. 1996

On the formation of longitudinal vortices in a turbulent boundary layer over wavy terrain.
J. Fluid Mech. **326**, 321-341.

Phillips, W.R.C., Wu, Z. and Jahnke, C.C. 1999

Longitudinal vortices in wavy boundary layers.
In: *Wind-over-Wave Couplings: Perspectives and Prospects*,
Sajjadi, S.G., Thomas, N.H. and Hunt, J.C.R. eds., pp.41-47.

Proctor, M.R.E. 1981

Planform selection by finite-amplitude thermal convection between poorly conducting slabs.
J. Fluid Mech. **113**, 469-485.

- Radder, A.C. 2001
Wind stress induced by sea waves. Werkdocument RIKZ/OS/2001.133x,
Rijkswaterstaat/RIKZ, October 2001, 33 pp. (Part 1)
- Sullivan, P.P. and McWilliams, J.C. 2002
Turbulent flow over water waves in the presence of stratification.
Physics of Fluids **14**(3), 1182-1195.
- Taylor, P.K. and Yelland, M.J. 2001
The dependence of sea surface roughness on the height and steepness of the waves.
J. Phys. Oceanogr. **31**(2), 572-590.
- Uz, B.M., Donelan, M.A., Hara, T. and Bock, E.J. 2002
Laboratory studies of wind stress over surface waves.
Boundary-Layer Meteorology **102**(2), 301-331.
- Vandemark, D., Mourad, P.D., Bailey, S.A., Crawford, T.L., Vogel, C.A., Sun, J. and Chapron, B.
2001 Measured changes in ocean surface roughness due to atmospheric boundary layer rolls.
J. Geophys. Res. **106** (C3), 4639-4654.
- Van Vledder, G.Ph. 1999
Source term investigation SWAN. ALKYON-report A162, July 1999, 83 pp.
- Young, I.R. 1998
An experimental investigation of the role of atmospheric stability in wind wave growth.
Coastal Engineering **34**, 23-33.